HIGH PERFORMANCE CONCRETE BRIDGES IN TENNESSEE

David Knickerbocker, Civil and Environmental Engineering, Vanderbilt University, Nashville, TN
Prodyot K. Basu, Civil and Environmental Engineering, Vanderbilt University, Nashville, TN
Mark Holloran, Tennessee Department of Transportation, Nashville, TN
Edward P. Wasserman, Tennessee Department of Transportation, Nashville, TN

ABSTRACT

Two double-span, jointless high performance concrete (HPC) bridges were thoroughly instrumented and tested during all phases of construction. Monitoring the performance of the bridges under environmental and operating conditions has been continued. The resulting field and laboratory test data were evaluated as per American Association of State Highway and Transportation Officials (AASHTO) codes and practices of the Tennessee Department of Transportation (TDOT), and good compliance was observed. A number of conclusions are made regarding material properties as well as method of construction.

Keywords: High Performance Concrete Bridges, Bridge Instrumentation and Monitoring, Concrete Material Testing, Tennessee Department of Transportation

BACKGROUND

Concrete materials technology has drastically improved in recent decades, opening the door to new opportunities for structural efficiency and durability of precast, prestressed concrete girder bridges. The ingredients and proportions of high performance concrete (HPC) are designed to achieve significantly higher strength and greater durability. Increased strength brings economy to highway bridge construction through allowance of fewer required girder lines, longer spans with corresponding reduction in number of intermediate supports, and decreased girder depth. Increased freedom in these design parameters can be exploited for ease in construction, as well as improved safety in service. The superior resistance of HPC to chloride ion penetration and freeze/thaw damage can be expected to reduce long-term maintenance costs and prolong bridge life.

With the authorization of the Transportation Equity Act of 1998 for the 21st Century (TEA-21), the Federal Highway Administration (FHWA) initiated the Innovative Bridge Research and Construction (IBRC) Program and provided funding for research and construction projects to demonstrate the applicability of HPC in bridge construction. Under FHWA's programs, a number of HPC showcase bridges have been built around the country[1]. The bridges have been instrumented following standard procedures[2] specified by FHWA for monitoring short- and long-term performance. Tennessee has been involved through research projects on showcase HPC bridges of its own, and construction of several bridges using HPC girders. This paper describes one such research project undertaken on two HPC bridges (Porter Road Bridge and Hickman Road Bridge) to perform material testing, bridge instrumentation, data collection, and interpretation and evaluation of results. The project involved collaboration among Tennessee Department of Transportation (TDOT) and FHWA, associated local contractors, and Vanderbilt. Greater detail of this study is available in a comprehensive report[3].

Tennessee's HPC showcase bridges, shown in Fig. 1, span across State Route 840 in Dickson County, TN. Design was carried out according to current TDOT practice, consisting of jointless cast-in-place deck slabs made continuous on precast, prestressed girders with

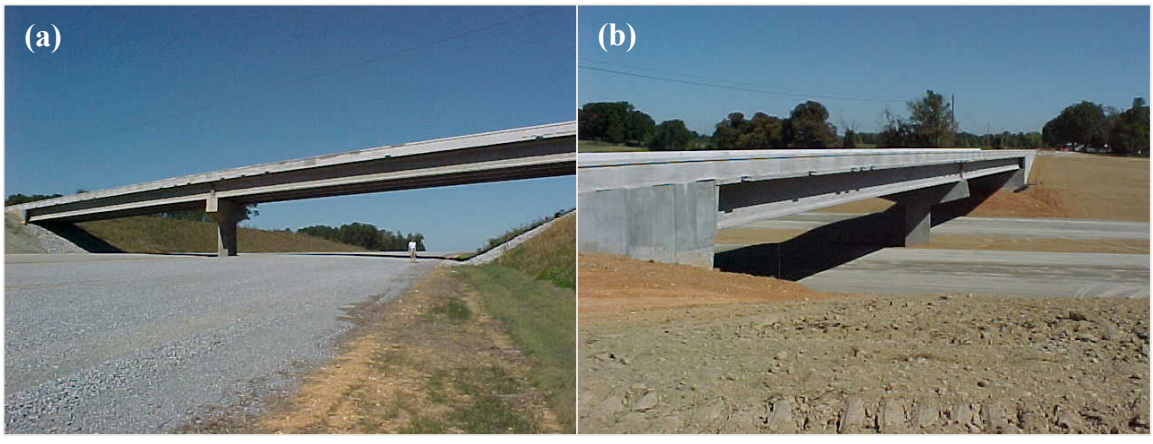

Fig. 1 Tennessee's HPC Showcase Bridges: (a) Porter Road Bridge; (b) Hickman Road Bridge

integral abutments. It is expected that this ideal combination of material and structural system will lead to more dramatic short- and long-term benefits. The two 159 ft (48.5 m) spans of the Porter Road Bridge are the longest of their kind built in Tennessee, thanks to the enhanced strength of HPC. Construction of the Porter Road Bridge was completed on May 15, 2000; the Hickman Road Bridge was finished on September 30, 2000.

Requirements for compressive strength of concrete were set at 10 ksi (68.9 MPa) for prestressed girders, 5 ksi (34.5 MPa) for cast-in-place deck slabs, and 4 ksi (27.6 MPa) for substructure. Maximum permeability ratings by the American Association of State Highway and Transportation Officials (AASHTO) Test Method T277 "Rapid Determination of the chloride Permeability of Concrete"[4] [American Society for Testing and Materials (ASTM) C1202 "Electrical Indication of Concrete's Ability to Resist Chloride Ion Penetration"[5]] were specified as 1,500, 2,000, and 4,000 Coulombs for slab, girder, and substructure concrete, respectively. Minimum density of cement was specified as 658 lb/cyd (390 kg/m^3) for both girder and deck HPC mixes. Also for both mixes, air content and slump were specified at 6±2% and 3±1in (7.6±2.5 cm), respectively. Finally, maximum allowed water-to-cementitious material (*w/cm*) ratio for both mixes was set at 0.43. Mix designs for girder and deck concrete are summarized in Table 1, from which the design *w/cm* ratio can be found to be 0.25 for girder, and 0.34 for deck concrete.

Table 1 HPC Mix Designs for Girders and Deck Slabs

MIX:		**GIRDER**		**DECK**	
Materials		**Density (U.S. Custom)**	**Density (Metric)**	**Density (U.S. Custom)**	**Density (Metric)**
Fine Aggregate		974 lbs./yd^3	578 kg/m^3	1116 lbs./yd^3	662 kg/m^3
Coarse Aggregate	#67	1439 lbs./yd^3	854 kg/m^3	1810 lbs/yd^3	1074 kg/m^3
	#11	481 lbs./yd^3	285 kg/m^3		
Cement Type I		747 lbs./yd^3	443 kg/m^3	494 lbs./yd^3	293 kg/m^3
Flyash Type C		249 lbs./yd^3	148 kg/m^3	154 lbs./yd^3	91 kg/m^3
High-range water reducer		5-15 ozs./yd^3	148-444 ml/m^3		
Silica Fume				50 lbs./yd^3	30 kg/m^3
Water		29.75 Gals/yd^3	147 l/m^3	28 Gals/yd^3	138 l/m^3
Remarks:		• Retarder to be added when ambient temperature is 75^{o}F or higher • Maximum slump not to exceed 8 in. or 200mm after addition of high-range water reducer		• Minimum f_c' = 5,000 psi on field report of concrete specimen	

STRUCTURAL DETAILS

Though reinforcement and prestressing details differ, the cross-sectional dimensions of the superstructures are identical; the typical cross-section is shown in Fig. 2. Four precast prestressed (strand diameter = 0.6 in., or 15.2 mm) 72 in. deep bulb-tee concrete girders (BT-72) per span, spaced on 100 in. (2.5m) centers, support a cast-in-place 8.25 in. (21.0 cm) deck slab. For pouring the deck, the gaps between girders are spanned by remain-in-place corrugated-steel-deck forms. Overall width of the deck is 32 ft (9.75 m). For superimposed dead and live loads, longitudinal steel reinforcement provides continuity in the deck over pier supports.

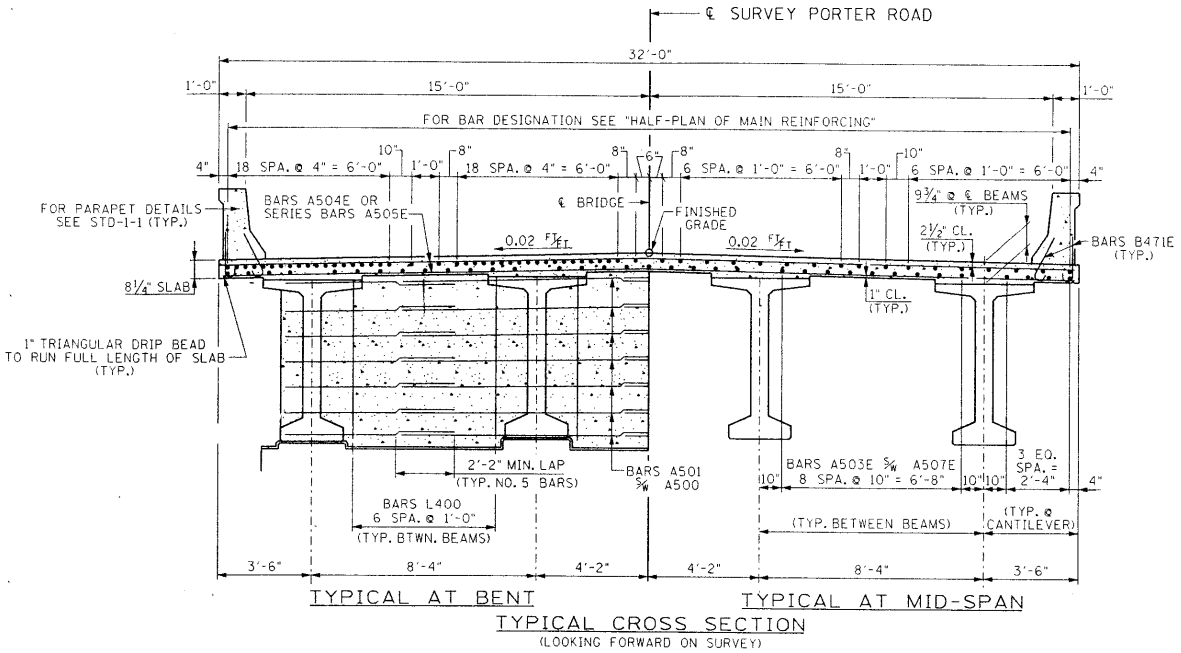

Fig. 2 Cross-Sectional Details of Porter Road Bridge Superstructure

Continuity is developed just after maturity of deck concrete, as deck slabs are poured monolithically with the diaphragms over the piers, and with abutment backwalls. Resistance to positive moment from creep and shrinkage of girders is provided by #5 (dia.=1.6 cm) rebars projecting from the girders into the diaphragms (or backwalls), and bent upward 90º. To increase the torsional stiffness of the deck, standard steel cross-bracing diaphragms are used in each span at third-points. The girders bear on ½ in. (1.3 cm) elastomeric pads.

The intermediate bents are built after the style of semi-rigid piers – designed to allow rotation and partially resist translation of the continuous deck. The diaphragm wall on the intermediate bent is anchored into it by means of standard anchor bolts, with freedom for differential rotation provided by ½ in. (1.3 cm) bituminous fiberboard at the pier-diaphragm interface. The piles supporting the abutments are placed in a single row (see Fig. 3) along

the skew to bend about their strong axis. These are embedded 1.0 ft (30.5 cm) into the abutment beams, with lengths varying according to geotechnical conditions. Each abutment has 12 ft (3.7m) wing walls of 23 in (58.4 cm) thickness adjoined by variable length (4-6 ft; 1.2-1.8 m) apron walls of 14 in. (35.6 cm) thickness. The differences in the characteristics of the two bridges are as follows.

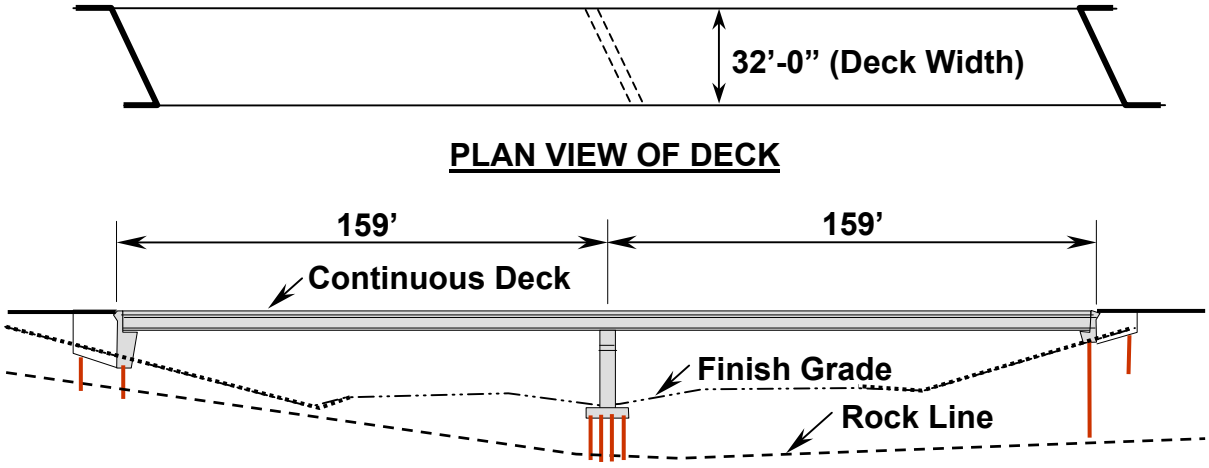

Fig. 3 Plan and elevation views of Porter Road Bridge

PORTER ROAD BRIDGE (BRIDGE #3)

The two-lane bridge has two spans of 159 ft (48.5 m) each with a 27º skew. As seen in Fig. 3, the two abutments differ significantly in size. The cross section of the abutment to the east measures approximately 4.5 ft (1.4 m) deep by 11ft (3.4 m) tall, while that of the west abutment measures about 4 ft (1.2 m) deep by 3.5 ft (1 m) tall. Each of the eight girders in the Porter Road Bridge is identical in design. In the cross-section shown in Fig. 4, each of the eight girders in Porter Road Bridge are pretensioned by fifty-four strands, out of which eight are debonded near the ends, and six are draped.

HICKMAN ROAD BRIDGE (BRIDGE #6)

The two-lane Hickman Road Bridge has an 18º-skew substructure supporting two spans of lengths 139.33 ft (42.5 m) and 151.33 ft (46.1 m). The roadway is on a slight vertical grade: 0.5%. Unlike those of the Porter Road Bridge, the abutments are of similar size, with cross-sections measuring approximately 5 ft (1.5 m) deep by 9.5 ft (2.9 m) tall. Each girder of the shorter span is prestressed by forty-two strands, out of which four are debonded near the ends, and two are draped, or raised toward the ends of the girder. In the longer span girders,

of which two have been instrumented, fifty strands are used for prestressing, 6 partially debonded and 6 draped (see Fig. 4).

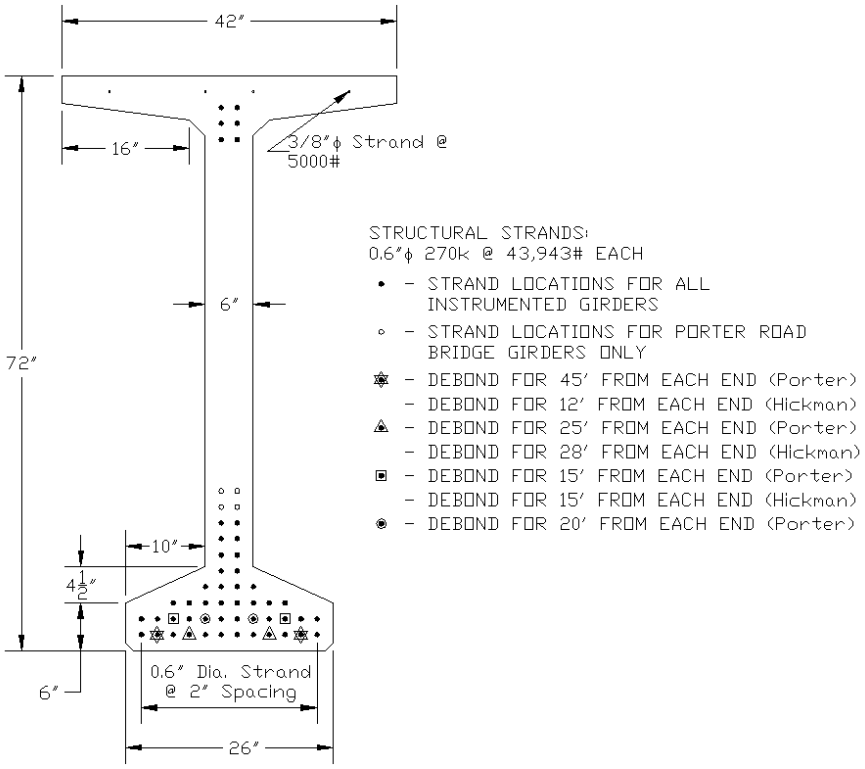

Fig. 4 BT-72 Girder Cross-Section, Showing Both Strand Patterns Used in Instrumented Girders

INSTRUMENTATION

For short- and long-term monitoring of prestressed girder and deck slab behavior, sensors and devices were installed as per FHWA guidelines[2] to measure

- Strains using embedded strain gages
- Temperature gradient using embedded thermocouples
- Girder camber and bridge deflection
- Slopes at bridge supports using digital tiltmeters
- Longitudinal abutment movement

The temperature and strain sensors were embedded in girders and deck slabs during the construction process. The instrumentation for camber and deflection measurements was installed after the pretensioned girders were cast and again after the deck construction was completed. Instrumentation for slope and abutment movement measurements was undertaken after the completion of construction. More in-depth details of the instrumentation are provided in a comprehensive report[3].

Two adjacent girders in each bridge, along with the overlying quadrant of deck slab, were instrumented in sections at midspan and at both ends of the span. In all, twelve sections of strain/temperature gages were thus installed in the two bridges, designated by: *P* (Porter Road Bridge), or *H* (Hickman Road Bridge); then *I* (interior beam), or *E* (exterior beam); and finally *a* (abutment end), *c* (center of span), or *b* (bent end).

Camber measurements were undertaken for the test girders immediately after release and subsequently in storage. Immediately after transfer, camber was measured directly from the casting bed. For subsequent camber and deflection measurements, a pulley and weighted string system was used. The integral abutments are designed to yield to the thermal expansion and contraction of the deck. On each abutment, thermal movements were periodically measured from a string line stretched parallel to the abutment face.

PROPERTIES OF HPC

The properties of concrete were measured during construction and at different stages of maturity to assess compliance by contractors as well as to compare with AASHTO code[6] provisions. Properties considered include compressive strength, tensile strength, modulus of elasticity, chloride ion permeability, and standard properties of fresh concrete mix. For creep and shrinkage properties, short and long-term measurements of the bridge behavior were relied upon. Various curing alternatives were used on the test cylinders for observation of their effects, including match-curing, steam curing, moist curing, and submerged curing at 100ºF. The results of the material testing program are summarized in Table 2.

Standard AASHTO Test Method T22 "Compressive Strength of Cylindrical Concrete Specimens"[4] (ASTM C39)[5] was used for testing compressive strength. Although a few of the compressive strength test results were below the 10,000 psi (68.9 MPa) threshold, and the average compressive strength at 28 days [$f_c^{'} = 10{,}377$ psi (71.6 MPa)] exceeded specifications by only 4%, compressive strength requirements for girder HPC were met overall. This adherence to specifications in compressive strength marks a success for the local concrete producers involved, especially considering that steam curing was used to achieve release strength of 8,000 psi (55.2 MPa) in 24 hrs. From Table 2, it can be seen that on the average, the girder concrete reached 92% of its 28-day compressive strength in 7 days, and an increase of only 7% is evident from the age of 28 days to that of 112 days. With regard to compressive strength of HPC used in the decks, all batches met the 28-day requirement of 5,000 psi (34.5 MPa) by a significant margin. Average strengths of the Porter Road Bridge deck concrete [$f_c^{'} = 8{,}265$ psi (57.0 MPa)] were notably greater than those of Hickman Road Bridge deck concrete [$f_c^{'} = 6{,}460$ psi (44.5 MPa)].

Table 2 Average Material Properties (n = number of tests performed)

Material Property	Mix: Age (days)	Girder n	Girder Average	Deck n	Deck Average
Compressive Strength	1	42	8,527 psi (58.8 MPa)		
	2	12	8,673 psi (59.8 MPa)		
	3	40	9,107 psi (62.8 MPa)		
	7	66	9,532 psi (65.7 MPa)	12	4,616 psi (31.8 MPa)
	14	66	10,249 psi (70.7 MPa)	6	5,685 psi (39.2 MPa)
	28	134	10,377 psi (71.5 MPa)	18	7,674 psi (52.9 MPa)
	35			6	7,402 psi (51.0 MPa)
	56	135	10,430 psi (71.9 MPa)	12	7,955 psi (54.8 MPa)
	84	24	11,040 psi (76.1 MPa)		
	112	24	11,103 psi (76.6 MPa)		
Permeability Rating	28	10	830 C	9	2,674 C
	S28*			3	317 C
	56	33	571 C	9	1,100 C
	S56*			3	269 C
Elastic Modulus	1	6	6,439 ksi (44.4 GPa)		
	3	10	6,797 ksi (46.9 GPa)		
	7	6	6,807 ksi (46.9 GPa)		
	14	6	6,702 ksi (46.2 GPa)		
	28	21	6,555 ksi (45.2 GPa)	12	4,494 ksi (31.0 GPa)
	56	15	6,546 ksi (45.1 GPa)	6	4,756 ksi (32.8 GPa)
Splitting Tensile Strength	1	12	820 psi (5.7 MPa)		
	3	6	835 psi (5.8 MPa)		
	28	18	912 psi (6.3 MPa)	12	756 psi (5.2 MPa)
	56	9	909 psi (6.3 MPa)	6	701 psi (4.8 MPa)
Slump	0	24	7.2 in. (18.3 cm)	6	4.5 in. (11.4 cm)
Unit Weight	0	24	153.5 pcf (2.4 kg/mm^3)		
Air Content	0	24	2.30%	6	4.60%
* − S Denotes Submergence at 100^{o}F Throughout Curing					

It is often practical to take note of relationships of compressive strength to modulus of elasticity, as well as to tensile strength. For modulus of elasticity testing, ASTM Test Method C469 "Static Modulus of Elasticity and Poisson's Ratio of Concrete in Compression"[5] was followed. The data collected on girder HPC in this study did not reflect a strong correlation of elastic modulus to compressive strength, nor to specimen age. Modulus of elasticity of girder concrete averaged 6,600 ksi (45.5 GPa). This value exceeds

predictions found in the literature[6-10] from $f_c^{'}$ of HPC and normal concrete. On the other hand, modulus of elasticity of deck concrete was in good agreement with the empirical prediction[8-9]

$$E_c = 10^6 + 40{,}000\sqrt{f_c^{'}} \quad (1)$$

in psi, based on $f_c^{'}$ of HPC.

Tensile strength was measured by AASHTO Test Method T198 "Splitting Tensile Strength of Cylindrical Concrete Specimens" [4] (ASTM C496)[5]. Tensile strengths both of girder and deck concretes were found to roughly follow the relationship

$$f_t = 8.8\sqrt{f_c^{'}} \quad (2)$$

Chloride ion penetration has been called the most devastating phenomenon to durability of concrete structures[10]. Ingress of chloride ions causes corrosion of reinforcing steel, and subsequent spalling of concrete, leading to further accelerated deterioration. For evaluating the HPC mixes' resistance against this mechanism, the rapid chloride ion permeability test[4,5] was used. As indicated in Table 2, the project specifications were met in this category. Girder concrete met specifications by a substantial margin at 28 days, while deck concrete met its requirement by 56-day age. Furthermore, submerged curing at 100˚F (38˚C) is shown to have a dramatic effect on permeability rating. It is illustrated in the plot of measured permeability rating vs. age of Fig. 5 that in all cases of chloride ion permeability tests, values decreased from concrete age of 28 to 56 days. It is interesting to note that a linear relationship was found between the 28-day rating for permeability and the rate of decrease over the next 28 days. Cylinders that were cured underwater at 100ºF showed significant lowering of permeability as compared to regular moist-cured specimens.

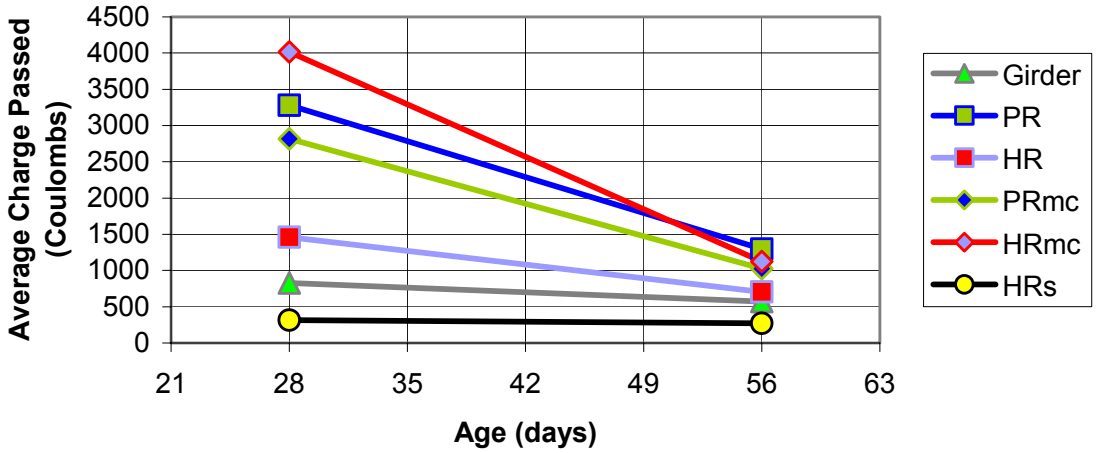

Fig. 5 Variation of Rapid Chloride Ion Permeability Rating with Specimen Age

PERFORMANCE OF PRECAST PRESTRESSED HPC GIRDERS

The performance studies included monitoring the thermal strains and deformation characteristics from the onset of pouring of concrete through transfer of prestress, storage, transportation, erection, pouring of deck to long-term behaviors under environmental and operating conditions.

CONSTRUCTION

The sixteen precast, prestressed, 72 in. (183 cm) bulb-tee girders used in the two bridges were manufactured by CPI of Memphis. Reusable segmental BT-72 steel forms were used on the casting beds, equipped with steam supply and "vibratrack" form vibrating system. According to a follow-up survey[11] and further correspondence with the manufacturer, the construction process for the HPC girders was the same as with conventional concrete, with a few minor differences. Indeed, most prestressing plants already produce concrete with low *w/cm* ratio, and high strength and durability. The movement toward HPC is accompanied by increasing quality control standards, such that the desired material performance parameters may be ensured.

In the survey[11], a few differences encountered in construction with HPC vs. normal concrete were mentioned. The increased concentration of cement, presence of super plasticizer and flyash, and specialized aggregate led to a material cost increase of 1.3 to 1.5 times that of normal concrete. Mixing times were slightly longer to ensure good dispersion of the high range super plasticizing admixture. To achieve the increased release-strength requirement of 8,000 psi (55.2 MPa), minimum duration of steam curing was set at 20 hrs, as opposed to the usual 14-16 hrs.

Overall, the conclusions drawn by the manufacturer were that HPC is easily mixed, placed, and finished, provided that good batch plant and quality controls are in place. In regard to assessment of concrete strength, the manufacturer emphasized that under factory environment, match curing of test cylinders is a favorable method. The Glenium-based super plasticizer used was found to facilitate easy placement of low *w/cm* ratio concretes. In fact, 3 years after the girders were cast, this admixture is now used in all of the mix designs produced at the plant.

As noted above, steam curing was used on the girders in order to ensure quick turnaround in manufacturing. Furthermore, the instrumented girders were cast during an extremely hot week in which daily high ambient temperatures exceeded 100˚F (38˚C), and nighttime low ambient temperatures were above 80˚F (27˚C). Embedded temperature gages in the girders reported maximum curing temperatures in the range of 150˚ – 173˚F (66˚ – 78˚C), with an average maximum temperature of 163˚F (73˚C).

LOSS OF PRESTRESS

It is well known that reduced creep and shrinkage, and increased elastic modulus of HPC lead to reduction in prestress losses. To assess the girder behavior in terms of losses, the embedded strain gages were used in four instrumented girders, one interior and one exterior girder in each bridge, defined as 3B1, 3C1, 6A2, and 6B2. Of interest are the ultimate strains induced by time-dependent effects of creep and shrinkage of concrete, and relaxation of steel; immediate strains induced at transfer and their implications on estimation of initial prestress force; and the estimation of prestress loss coefficient, η, which is the ratio of prestress force after all losses to the initial prestressing force.

In the analysis of prestress losses for a specific case, knowledge of the particular sequence of loading is imperative. Following is an overview of the sequence followed for the 4 girders studied. Strain values of interest are compiled in Table 3; strain parameters appearing in the table are defined subsequently. Likewise, Table 4 presents the relevant prestress force parameters.

The design prestress load P_D is the total prestress force designated to be "transferred" at release. Using the ratio of applied prestress to ultimate stress for the strand material, $f_{pi}/f_{pu} = \frac{202.5}{270} = 0.75$, along with the total area of all prestressing strands used in a section, P_D can be obtained. To compensate for the losses in prestress from anchorage seating, friction, abutment movements, and temperature; an augmented force, P_G, is applied such that it reduces to P_D as the initial seating losses take effect. These estimated losses that occur before casting are denoted by L_A.

Table 3 Strains Used in Calculations of Prestress Losses (x 10^{-4})

Section		$(\varepsilon_T)_o$	$(\varepsilon_T)_e$	ε_Y	ε_{CS}
3B1	a	-3.655	-6.092	-7.412	NA
	c	-4.586	-6.280	-8.080	NA
	b	-3.724	-5.975	-7.275	NA
3C1	a	-4.076	-6.408	-7.550	NA
	c	-5.068	-6.760	-7.890	NA
	b	-3.909	-6.451	-7.615	NA
6B2	a	-3.321	-6.672	-8.001	NA
	c	-4.318	-6.757	-7.660	-10.560
	b	-3.319	-6.538	-7.636	-10.236
6A2	a	-3.468	-6.594	-7.752	-10.052
	c	-4.419	-6.734	-7.765	-10.465
	b	-3.397	-6.356	-7.566	-10.266

Table 4 Cumulative Prestress Forces and Incremental Losses (kips) Found at Instrumented Sections of 4 Girders, and Prestress Loss Coefficient η

Section		P_G	L_A	P_D	P_i	L_{ES}	P_T	$\bar{L}_Y$	P_Y	L_{CS}	P_{CS}	η
3B1	a	2147	-126	2021	2092	-173	1920	-37	1882	*NA*	*NA*	*NA*
	c	2521	-148	2373	2618	-209	2409	-60	2349	*NA*	*NA*	*NA*
	b	2147	-126	2021	2125	-169	1956	-37	1919	*NA*	*NA*	*NA*
3C1	a	2147	-126	2021	2240	-181	2058	-32	2026	*NA*	*NA*	*NA*
	c	2521	-148	2373	2784	-225	2559	-38	2522	*NA*	*NA*	*NA*
	b	2147	-126	2021	2157	-183	1974	-33	1941	*NA*	*NA*	*NA*
6B2	a	2037	-104	1933	1823	-181	1642	-36	1606	*NA*	*NA*	*NA*
	c	2315	-118	2197	2343	-208	2135	-28	2107	-89	2018	0.87
	b	2037	-104	1933	1818	-177	1641	-30	1611	-70	1541	0.86
6A2	a	2037	-104	1933	1812	-179	1633	-31	1602	-62	1540	0.87
	c	2315	-118	2197	2289	-207	2081	-32	2050	-83	1967	0.87
	b	2037	-104	1933	1772	-172	1600	-33	1567	-73	1494	0.86
		L_A/P_G			L_{ES}/P_i		$\bar{L}_Y/P_T$		L_{CS}/P_Y			Average
Average %:		5.5			8.8		1.8		4.2			0.87

Again, this investigation is based on readings from the embedded strain gages. No relevant information is available from these gages until the instant of prestress transfer. At that time, the force applied to the girder P_T can be computed from the strain $(\varepsilon_T)_o$ at the centroid of the gross concrete area as

$$P_T = (\varepsilon_T)_o \, E_{cT} \, A_c \tag{3}$$

where E_{cT} = Elastic Modulus of concrete at transfer, and A_c = 767 in^2 (4948 cm^2) = gross cross-sectional area of girder. Average values for E_{cT} were obtained experimentally as per ASTM C469[9] at the time of transfer [3B1 – E_{cT} = 6,848 ksi (47.2 GPa); 3C1 – E_{cT} = 6,584 ksi (45.4 GPa); 6B2 – E_{cT} = 6,447 ksi (44.5 GPa); 6A2 – E_{cT} = 6,141 ksi (42.3 GPa)].

At transfer of prestress, the losses L_{ES} associated with elastic shortening occur immediately. L_{ES} is found from the strain $(\varepsilon_T)_e$ at the level of the prestress force resultant by

$$L_{ES} = (\varepsilon_T)_e \, E_{ps} \, A_{ps} \tag{4}$$

in which E_{ps} = elastic modulus of prestressing steel = 28,500 ksi, and A_{ps} = n (0.216 in^2/strand) = area of prestressing steel (n = 54 for 3B1, 3C1 and 50 for 6A2, 6B2). With immediate losses L_T and prestress force after transfer P_T, the force before transfer P_i can be approximated by

$$P_i = P_T - L_{ES} \tag{5}$$

Noting that L_{ES} will be negative, P_i is larger than P_T and should be compared to the design P_D value.

After transfer, the girders were moved into storage, where the supports were located some distance from the ends (13 ft (4.0 m) for Porter Road Bridge girders, and 7 ft (2.1 m) for Hickman Road Bridge girders). This decreases the positive moment resulting from member weight, thereby shortening the strands by increased negative bending, and decreasing the prestress force to P_Y. The elastic decrease in prestress designated as $\bar{L}_Y$, is not a loss in that it is recoverable when the girder is placed on (pier and abutment) end supports. It is quantified so that its effect can be removed from loss calculations. Moreover, the increased negative moment that results from the revised support condition tends to increase the magnitude of creep encountered by the girder during storage. The above quantities are related by

$$\bar{L}_Y = [\varepsilon_Y - (\varepsilon_T)_e] E_{ps} A_{ps} \tag{6}$$

and

$$P_Y = P_T - \bar{L}_Y \tag{7}$$

with ε_Y = strain at centroid of strands immediately after placement in the storage yard.

Besides the support conditions, another influence on strain to be considered is the effect of temperature variation along the depth of the member with time. In observing prestress losses via strain data, it is desirable to eliminate the effects of temperature variations on the strain. Accordingly, the effects of temperature were estimated and subtracted from the strain data. The remaining strain constituted the immediate strain due to prestress load, and time dependent effects of shrinkage, creep, and relaxation.

Strains developed at strand centroid levels with the passage of time were recorded and corrected for temperature effects, beginning immediately after placement in the storage yard. Hickman Road Bridge girders remained in the yard for nearly eight months, and it was noted that most of the time-dependent effects occurred during this period. This analysis could not be applied to the Porter Road Bridge girders (3B1, 3C1), as the girders remained in storage for only about two weeks.

Strains ε_{CS} were recorded at the level of prestress force resultant after the apparent effects of creep, shrinkage, and relaxation had leveled off. The associated losses L_{CS} can be calculated using

$$L_{CS} = [\varepsilon_{CS} - \varepsilon_Y] E_{ps} A_{ps} \tag{8}$$

giving the residual prestressing force as

$$P_{CS} = P_Y - L_{CS} \tag{9}$$

Again, the immediate effects of changed support conditions in the storage yard are reversible, thus the prestress force, upon delivery of the girder to the bridge, is expected to be

$$P_F = P_{CS} + \overline{L}_Y \tag{10}$$

This final prestress force P_F is not verifiable by the strain gage data, as the data loggers were not reinstalled at the bridges until just before pouring of the deck, after substantial loads from forms and deck steel had already been placed on the girders.

The prestress loss coefficients were obtained from

$$\eta = \frac{P_i + \left(L_T + L_{CS}\right)}{P_i} \tag{11}$$

Because of the construction schedule involving instrumented girders 3B1 and 3C1, necessary strain data for estimation of time-dependent losses were not available. The data that was available from these girders, however, is in agreement with that taken from the other girders, 6A2 and 6B2. Given that all girder concrete material is of the same mix design and treated under the same methods of structural design, with only small discrepancy in length and corresponding moment considerations, it is reasonable to conclude that for all girders studied, the coefficient of prestress losses η is 0.87.

CAMBER

Predictions of camber were made numerically using the following assumptions. In a free beam, the curvature caused by loading is

$$\phi(x) = \frac{M(x)}{E_g I_g} \tag{12}$$

where $M(x)$ is the applied moment as it varies with longitudinal distance x, and E_gI_g is the beam bending stiffness. Any additional curvature is caused by factors other than load, such as temperature, creep, or shrinkage. Once the curvature is obtained as a function of x along beam length, the slope can be obtained from

$$\theta(x) = \int \phi(x)dx \tag{13}$$

Finally, deflection is calculated as

$$\delta(x) = \int \theta(x)dx \tag{14}$$

The deflection can be obtained at any point along the beam if the moment diagram is known. Based on the above relationships, analyses were performed for all stages of interest in the life

of the girder, from prestress transfer to application of deck weight. Results therefrom are presented in Table 5. The measured values of initial camber were over-estimated by about 1¼ in. (3 cm). Later camber measurements were, however, slightly underestimated by the predictions.

Table 5 Measured Camber with Analytical Predictions (in.)

Age (days)	3B1		3C1	6A2		6B2
	Experimental	Analytical	Experimental	Experimental	Analytical	Experimental
1 (Release)	3	4.22	2.5	3.1	4.31	3.1
3		5.18			4.67	
7			5.7			
8	5.4					
11				5.1		5.5
13			5.3			
14	5.3		5.2			
15	5.2					
18				4.5		4.7
28				4.6		5.0
32				5.2		5.3
42				5.3		5.6
56		5.31		5.6	4.80	5.5
70				5.3		5.2
84				5.2		5.2
97				5.2		5.1
112				5.1		5.1
117				5.6		5.7
143				5.5		5.5
172				6.0		6.0

Thermal Effect on Camber

A case of temperature change from morning to afternoon of a particularly hot day was analyzed for appreciation of thermal effects on camber. The nonlinear thermal gradients of temperature difference in each of the four girders studied approached 40ºF (22ºC) at the top, and only about 5ºF (3ºC) at the bottom. The curvatures imposed by these gradients correspond to average change in camber of 0.76 in. (1.9 cm). This is a substantial percentage of the initial measured cambers of 2.5-3 in. (6.4-7.6 cm).

STUDIES OF BRIDGE SYSTEM

After the girders were erected in place, the deck was poured in-situ using stay-in-place corrugated metal forms. The following studies refer to the resulting bridge system in terms of material behavior as well as short- and long-term response to environmental and operating conditions.

DECK PLACEMENT AND CURING

Cast-in-place deck slabs are particularly of interest in high performance concrete bridge construction, where demands of surface finish and long-term durability are contrasted with the quality control limitations of in-situ concrete construction. The placement of HPC decks for highway bridges is presently carried out using experience and equipment developed over time for normal concrete. The pertinent question is whether the existing skills and tools are optimal to produce required density and finish with the more advanced concrete mixes. One of the motivations for this study was to get an idea of local contractors' abilities to place and finish HPC. Toward that objective, an account of the experience of construction personnel with in-situ HPC construction has been recorded from the contractor and from the resident engineer representing the state. The contractor and the engineer agreed that the main problem they faced was that the concrete mix was stickier than usual, and adjustment of the finishing process was required.

The Porter Road Bridge deck was placed on January 19, 2000 with ambient temperatures ranging between 35 and 40ºF (1.7-4.4ºC). It was noted that, due to stickiness of the concrete mix, ridges formed perpendicular to the roadway. As the screed pan passed along the surface of the mix, it tended to adhere to the concrete, creating a pulling action. Also, it was noted that some pulling up of the aggregates did occur. It was felt that these problems were caused by lack of bleed water.

The Hickman Road Bridge deck was placed on May 19, 2000, when the temperature was about 70ºF (21.1ºF). Based on the experience gained from the PR Bridge deck placement, measures were taken to ensure ample bleed water during the curing process. Extra fogging was applied to the slab until it could be covered with water-soaked burlap. Fogging refers to maintenance of moisture on the slab through use of pressure washers. This required four extra laborers and two pressure washers. The size of the ridges that formed from the screed was thereby reduced, and the problem of aggregate pulling was eliminated.

Because of the more critical role of water in the curing process, moisture curing was continued on both deck slabs (with burlap) for 7 days rather than the usual 5. In general, it was noted that at high ambient temperatures, setting time is more rapid for HPC than for normal concrete. At low temperatures, a difference in curing time was not noticeable. Strength was noted by the project engineer to have increased by about 50% above the values expected with normal concrete.

Overall, it is the opinion of the construction officials that HPC in bridge decks brings advantages of higher strength and faster setting and curing times. The tradeoff for these advantages is a more labor-intensive process. The quality of the decks was found to be acceptable; permeability and strength requirements were adequately met in lab tests. Also, the finish of the decks is without any cracking to speak of, despite any lack of bleed water, and therefore can be expected to resist wear/scaling and penetrating agents reasonably well. Some respondents expressed concerns about the driving surface, which is affected by the small ridges that formed from the concrete's adhesion to the screed. The general feeling is that after sufficient time for necessary experience of the personnel with the new material, these issues of placement and surface finish will be completely resolved. Indeed, progress has been made during the construction of these two bridges.

Low permeability provided by HPC is desired to counteract the electrochemical corrosion that occurs in steel reinforcement. This corrosion is in large part a result of presence of chloride ions introduced by de-icing agents, mixing water, or other sources. When properly engineered, concrete decks are placed under high quality-control conditions, the alkalinity of the concrete is effective in resisting the chloride ion corrosion[12]. Cracking problems have arisen due to restraint to thermal and shrinkage contraction, as well as the characteristic high elastic modulus and low creep coefficient of HPC[13,14]. The deck concrete was engineered and produced to meet the chloride ion permeability requirements. However, if the deck concrete is prone to cracking due to other causes, the steel may once again be vulnerable to harmful chlorides.

THERMAL EFFECTS

Internal temperatures were recorded on a hot afternoon when the ambient temperature was about 100ºF (38 ºC). Temperatures on top of the deck were measured with a handheld digital thermometer, and temperatures at the bottom of the section were estimated by linear extrapolation of sensor data. Comparison of AASHTO design thermal gradient[7] to measured temperature profiles showed good agreement.

As expected in jointless bridge design, the integral abutments were found to be sufficiently flexible to allow longitudinal movements of the superstructure in response to temperature change. However, the rotational tendency at the ends caused by steep thermal gradient in the superstructure was constrained by the substructure. As a result, girder moments at the abutment and pier resulting from average internal temperature change of 50ºF (28 ºC) were found to be on the order of 1000 kip-ft (1.4 MN-m). Such moments may need to be accounted for in the design.

CREEP AND SHRINKAGE

Early-age shrinkage and creep impose negative axial and bending deformations on prestressed concrete girders. For prestressed concrete superstructures made continuous, cracking at the diaphragm due to the resulting positive moment above the bent is a cause of

concern[15], especially as span lengths are likely to be increased with higher concrete strength. To circumvent this problem, Tennessee requires that prestressed girders should achieve an age of 90 days before enforcing continuity with deck/ diaphragm casting. Recorded histories of strain in the instrumented girders demonstrated that this period of time before deck casting is adequate in stabilizing the effects of creep and shrinkage in the girders.

The effects of creep and differential shrinkage resulting from pouring of the deck were observed through strain data with thermal effects removed. It was found that small tensile strains were introduced in the top of the deck above the pier due to time-dependent effects. Assessment of vulnerability to cracking at this location is complicated, as the strains measured do not truly relate to stress, which would be useful in comparison with modulus of rupture. Under shrinkage, the dimensions of the concrete member are decreased, introducing a "compressive" deformational strain. Translating the measured tensile strain to stress by the modulus of elasticity would then be ignoring the stress that was required to overcome the compressive time-dependent free strain. As the creep and shrinkage parameters of the HPC in this project are not known with precision, and because the deck above the pier is also susceptible to tensile stresses due to live load and negative temperature gradients, it may be of interest to study this matter of deck cracking further, in the interest of long-term durability.

CONCLUSIONS

Overall, girder compressive strength results satisfied the 28-day requirement of 10,000 psi (68.9 MPa). Compressive strengths of the deck HPC mix met requirements by a substantial margin. Chloride ion permeability rating requirements were met for all batches tested, with deck concrete requiring 56-day maturity to make the grade. Submerged curing showed dramatic improvement in permeability rating. Based on the splitting tensile strength test results of both girder and deck concrete specimens, the variation of tensile strength with compressive strength is proposed as

$$f_t = 8.8\sqrt{f_c'} \tag{2}$$

in units of psi.

By following normal construction practices under Tennessee conditions it was possible to successfully build the two HPC bridges. The difficulties in getting good finish to the deck concrete have been experienced in other states as well. The use of HPC was found to be beneficial to jointless construction due to increased strength. Indeed, the Porter Road Bridge carries the longest prestressed concrete bridge spans built as yet in the state; thanks to the superior properties of HPC, the required number of intermediate supports was reduced. Enhanced durability is expected to pay off as well, particularly with respect to bridge decks.

REFERENCES

1. Miller, R. A. PCI Committee Report: High Performance Concrete Showcase Bridges. *PCI Journal*, Vol. 46, No. 6, November-December 2001, pp. 42-55.
2. Russell, H. G. *Implementation Program on High Performance Concrete – Guidelines for Instrumentation of Bridges*. Report FHWA-SA-96-075. FHWA, U.S. Department of Transportation, 1996.
3. Basu, P. K., and D. J. Knickerbocker. *High Performance Concrete Bridges*. TDOT Report TNSPR-RES1162. Department of Civil and Environmental Engineering, Vanderbilt University, 2002.
4. AASHTO STANDARD SPECIFICATIONS FOR TRANSPORTATION MATERIALS AND METHODS OF SAMPLING AND TESTING: PART II TESTS-Nineteenth Edition. American Association of State Highway and Transportation Officials, Washington, DC, 1998.
5. ASTM Annual Book of Standards, Volume 4.02 Concrete and Aggregates. American Society for Testing and Materials, Philadelphia, PA, 1998.
6. AASHTO. LRFD Bridge Design Specifications, Customary Units - Second Edition, American Association of State Highway and Transportation Officials, 1998.
7. ACI. Building Code Requirements for Structural Concrete (ACI 318-99) and Commentary (ACI 318R-99). American Concrete Institute, Farmington Hills, MI, 1999.
8. Nawy, E. G. *Fundamentals of High Strength High Performance Concrete*. Longman Group Limited, London, 1996.
9. Nilson, A. H. *Design of Prestressed Concrete, Second Edition*. John Wiley & Sons, Inc., New York, 1987.
10. Aïtcin, P.-C. *High-Performance Concrete*. E & FN Spon, New York, 1998.
11. Maybee, A. (2002). "HPC Questiuonnaire: TDOT/FHWA HPC Bridge Construction Project." V. U. Department of Civil and Environmental Engineering, ed., Concrete Products, Inc., Nashville, TN.
12. Burke, N. D., and J. B. Bushman. *Corrosion and Cathodic Protection of Steel Reinforced Bridge Decks*. Report FHWA-IP-88-007, Federal Highway Administration, U.S. Dept. of Transportation, 1988.
13. Pfeifer, D. W. State of the Art Paper: High Performance Concrete and Reinforcing Steel with a 100-Year Service Life. *PCI Journal*, Vol. 45, No. 3, May-June 2000, pp. 46-54.
14. Krauss, P. D., and E. A. Rogalla. *Transverse Cracking in Newly Constructed Bridge Decks*. NCHRP Report 380, NCHRP, 1996.
15. Ma, Z., X. Huo, M. K. Tadros, and M. Baishya. Restraint Moment in Precast/Prestressed Concrete Continuous Bridges. *PCI Journal*, Vol. 43, No. 6, November-December 1998, pp. 40-56.